

N.M. RAFIYEV, V.I. AHMADOV, A.A. ISAYEVA

Azerbaijan University of Architecture and Construction
(Ayna Sultanova 11, Baku AZ1073, Azerbaijan)

PROSPECTS TO USE AMORPHOUS Fe–Ni–Si–B RIBBONS IN CONTACTOR CORES

UDC 539

We consider the possibility to use an amorphous Fe–Ni–Si–B material in the core of contactors, which are widely used in connecting and disconnecting electric circuits, instead of the crystalline material of 3% electric steel. Alloys containing Fe–Ni–Si–B have been treated with the use of mechanical, thermomechanical, and magnetic fields, and the material for practical applications has been obtained. The processing modes were chosen so that a change in the performance of ferromagnetic (below the Curie temperature) alloys during the annealing could be controlled. The obtained specimens were annealed in oil at 360 °C in a magnetic field of 200 A/m for 200 min. The temperature mode was chosen so that the stress relaxation could occur during the annealing, and the structural changes in the material could be observed.

Keywords: amorphous magnetic alloy, processing.

1. Introduction

Electric and magnetic properties of amorphous alloys are of greater interest than other ones, because amorphous materials surpass their crystalline counterparts in practical applications [1]. To date, numerous studies have been carried out to investigate the magnetic properties of amorphous materials. Currently, amorphous magnetic materials have found a wide range of practical applications [2, 3, 4, 5]. The modern rapid development of the electronics and the device manufacturing industry increases the demand for materials with affordable and new properties. In this sense, the aim of research on amorphous magnetic materials is to reveal more suitable properties of these materials. In this work, we consider the possibility for amor-

phous Fe–Ni–Si–B materials with favourable magnetic properties, high electric resistance, low losses, and high corrosion resistance to replace crystalline contactor cores made of 3% electric steel. AC powered, Siemens 3Tf43-10 brand cores, which are made of 3% electric steel, of the temperature-control contactor of the equipment were replaced with new amorphous cores made of the studied specimens and tested in operation.

The reason for this replacement is the rapid failure of the existing crystal contactors during their operation. Observations made in the production area show that the reasons for the frequent failure of the existing contactors during the operation are as follows:

- Heating and failure of contact parts due to eddy current losses during the remagnetization.
- Loss of the conductivity of contact parts due to the corrosion.
- Damage of the contact ends due to the impact during connections.

Different concentrations of elements in the chemical compositions of the materials, and the application of different processing modes are considered

Citation: Rafiyev N.M., Ahmadov V.I., Isayeva A.A. Prospects to use amorphous Fe–Ni–Si–B ribbons in contactor cores. *Ukr. J. Phys.* **68**, No. 3, 201 (2023). <https://doi.org/10.15407/ujpe68.3.201>.

Цитування: Рафієв Н.М., Ахмадов В.І., Ісаєва А.А. Перспективи використання аморфних Fe–Ni–Si–B стрічок у серцевинах контакторів. *Укр. фіз. журн.* **68**, №3, 201 (2023).

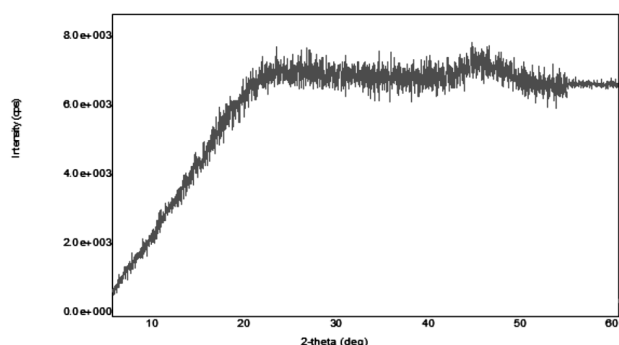


Fig. 1. X-ray diffraction spectrum of the specimen

to be the main factors that favourably change the properties of amorphous magnetic materials [6, 7]. In [8], by applying different processing modes, soft magnetic materials with the coercive force value of $H_c = 10$ A/m were obtained in ribbon-shaped specimens containing $Fe_{56}Co_7Ni_7B_{20}Nb_{10}$. In [9], it was shown that the addition of 2% Mo reduces the coercive force from 100 A/m to 5 A/m in amorphous $Fe_{75}Mo_2Ga_3P_{10}C_4B_4Si_2$ alloy. In [10], it was determined that Ni in the composition has a strong in-

Table 1. Chemical composition of FeSi compound

s/s	Chemical element	Symbol	Atomic concentration, %
1	Aluminum	Al	0.716
2	Silicon	Si	74.502
3	Phosphorus	P	0.016
4	Sulphur	S	0.004
5	Calcium	Ca	0.113
6	Titan	Ti	0.064
7	Chromium	Cr	0.021
8	Manganese	Mn	0.063
9	Iron	Fe	24.501

Table 2. Chemical composition of FeB compound

s/s	Chemical element	Symbol	Atomic concentration, %
1	Boron	B	18
2	Silicon	Si	4 max
3	Carbon	C	0.8 max
4	Sulphur	S	0.001 max
5	Phosphorus	P	0.002 max
6	Iron	Fe	76.7
7	Aluminum	Al	0.5 max

fluence on the magnetic properties and is the main factor to get soft magnetic properties, by creating an anisotropy field and reducing the coercive force. The authors of [11] found that processing of amorphous $Fe_{80}B_{20}$ alloy at 449 °C worsens the soft magnetic properties and leads to an increase in the coercive force. As can be seen from numerous studies, the choice of a chemical composition and a processing mode is the main factor to obtain various required magnetic parameters depending on the purpose.

2. Materials and Methods of Experiment

In the research, the materials used as starting raw materials in the synthesis of alloys were obtained from the “Baku Nonferrous Metals and Ferroalloys Company” LLC plant located in Sumgayit, Azerbaijan Republic. The FeSi compound was used as a source of iron and silicon. The chemical composition of the FeSi compound is presented in Table 1. Fe, Ni, and B elements used in the research were obtained from Sigma Aldrich, Germany and FeB from Inner Mongolia Pusheng Iron & Steel Co LLC, China. The chemical composition of FeB compound is shown in Table 2. Amorphous ribbons were obtained using a device for the annealing from the liquid state developed in the scientific-research laboratory “Physics of Metals and Alloys” of the Azerbaijan University of Architecture and Construction. Through a refractory crucible placed in the induction furnace equipped with a high-frequency generator, the pre-prepared $Fe_{39}Ni_{39}Si_9B_{13}$ alloy was heated to a melting temperature of 1650–1700 °C and directed to the cooling drum through a slot opened from the bottom of the crucible.

The metal flow hits the copper drum and solidifies at a very high speed. At this time, a cooling rate was 10^5 – 10^6 K/s. Such laminar flow allows the formation of a homogeneous ribbon with a constant thickness. The whole process was carried out in an inert gas atmosphere. In this study, amorphous ribbons with a width of 15 mm and a thickness of 30–50 μ m were obtained by the melt spinning method. The output nozzles are 4.2×1.8 mm in size. The calculated cooling rate for this alloy was 4.2×10^5 K/s.

The amorphous structures of the metal ribbons of different compositions were determined by the X-ray diffraction (XRD) analysis (Fig. 1). A Shimadzu XRD 6000 diffractometer was used for this purpose. Measurements were performed in copper radiation ($CuK\alpha_1 = 1.54056$ E) at 40 kV and 30 mA.

Determination of magnetic indicators was carried out on an EZ-VSM vibration magnetometer with the highest electromagnetic base up to 3 T.

The specific electric resistance was determined by a high-precision Micro-Ohmmeter MICO-21. The Voltmeter-Ammeter-Wattmeter method was used to determine the eddy current losses [22]. Plastic deformation was performed on a testing machine AL-CEK-21P and a rolling device EZM 50 shown in Fig. 2 was used for the ribbon rolling. With this device, it is possible to roll the ribbons by compressing them with a pressure up to 1 MPa.

One of our main tasks is to identify the features of the structure formation, the effect of this structure on physical properties and to propose new processing modes with complex thermomechanical effects on the material.

Figure 3 shows the manufacturing process of the contactor core and its dimensions. Amorphous ribbons of the contactor core are made in the size of $44 \times 18.5 \times 12$ mm and were 12 mm wide and 0.03 mm thick. First, two specimens of an ellipsoid shape with a diameter of 29 mm were prepared from a set of amorphous tapes wound on the top of each other. The set was 4 mm thick. Then a specimen was obtained by touching them to each other and winding new ribbons on them. The thickness of the set was also 4 mm. When the ribbons are wound, they are insulated with appropriate lamination materials. After the process of extracting the inserts from the center of the specimen, two contactor cores were obtained, being divided into two parts by the method of cutting the conductor.

The processing modes were chosen so that a change in the performance of ferromagnetic (below the Curie temperature) alloys during the annealing could be controlled. The obtained specimens were annealed in oil at 360 °C for 200 min. The annealing process was carried out in a magnetic field of 200 A/m. The low temperature (240 °C) was chosen so that the stress relaxation could occur during the annealing process, and the structural changes of the material could be observed.

3. Discussion of the Work

The contactor cores, which are the object of the research, are heated up due to the passage of the electric current during the operating process, in connecting and disconnecting electric circuits, and the end



Fig. 2. Rolling device EZM 50 for the deformation of amorphous ribbons by rolling

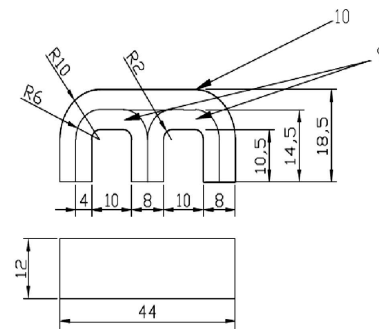


Fig. 3. Amorphous core shapes and sizes

parts are corroded by environmental influences and deformed due to the impact during connections. This leads to the malfunctioning of operators due to phase interruptions and the disruption of the operating mode. To avoid these difficulties, the deformation and temperature dependence of magnetic properties of the studied material have been considered. As can be seen from Fig. 3, the maximum magnetic induction B_m value decreases with increasing deformation, while the value of the residual magnetic induction B_r , B_r/B_m ratio and the coercive force H_c increase. However, these changes are expressed in very

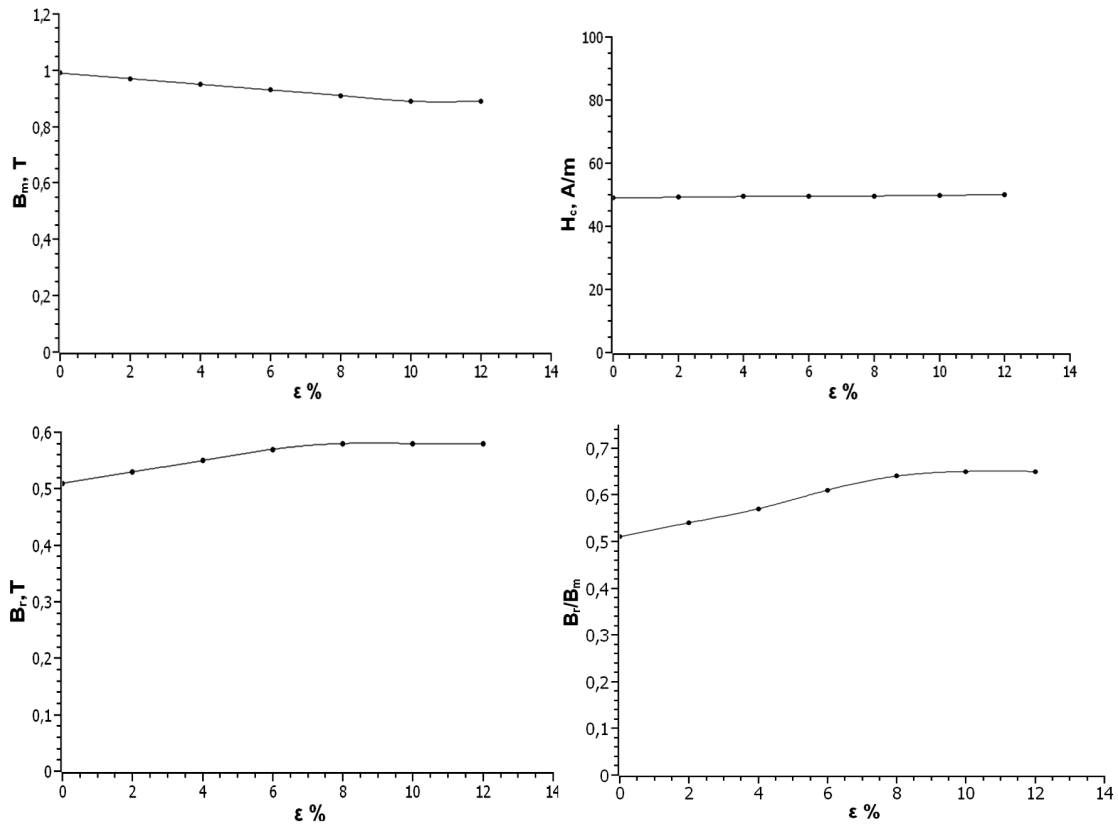


Fig. 4. Dependence of magnetic properties on the deformation in $\text{Fe}_{39}\text{Ni}_{39}\text{Si}_9\text{B}_{13}$ alloy

low values and hardly affect the technical properties of the material. The change in the magnetic properties B_r and H_c during a deformation can be explained by the effect of the elastic stress field. This fact is reflected in the dependence of the mentioned parameters on the deformation degree. It is believed that the formation of the mechanism of increase of B_r can be caused by the mechanism of pair atomic arrangement during the development of small deformation changes of the material, as well as the exit of free volume and the movement of sliding zones [12, 24].

Figure 4 shows the dynamics of changes in magnetic parameters during the processing by annealing after a 5% deformation in the low temperature region (240 °C). The nature of changes in B_m and H_c during the annealing corresponds to the dynamics of the relaxation of stresses. This also indicates that the change of the values observed during the deformation is related to the formation of additional stresses in the cross-section of the ribbon. As can be seen, the value of B_m mainly changes in the initial stage of anneal-

ing. The value of H_c changes more dramatically in the initial stage of annealing. At the subsequent temperatures, the value of H_c decreases slightly (Fig. 4). The characteristic values for B_r do not change significantly during the annealing. According to the corresponding hypothesis, the change in B_r is not due to additional elastic deformation stresses, but mainly to atomic ordering processes [13]. The results of the analyses show that the influence of the stress on the magnetic properties is low. This is indicated by a small change in the dependence of B_r on the annealing time. As can be seen from Fig. 4, when the material is deformed by 5%, the influence of the processes at the atomic level is noticeable, and the relaxation processes start to proceed slowly.

This is due to elastic stresses. The B_r/B_m ratio depends on the change of B_m and B_r and its value decreases during the annealing, but not as intensely as B_r .

The change of the magnetic properties of the material after a plastic deformation by rolling at a pres-

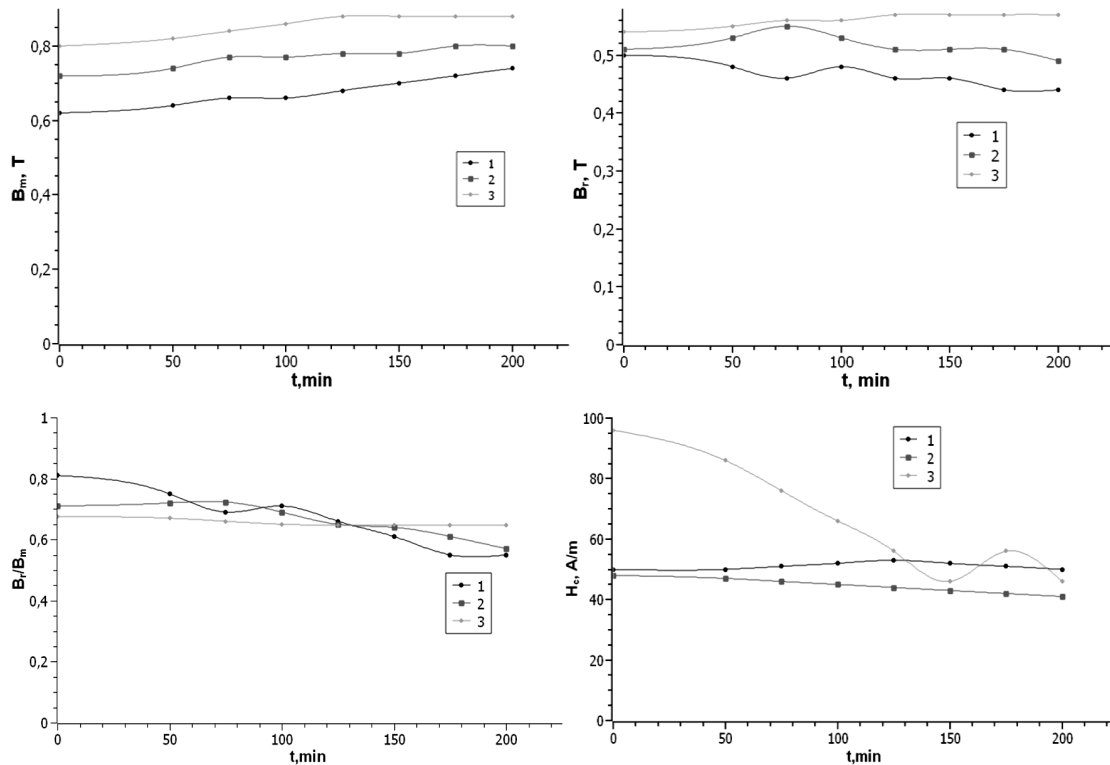


Fig. 5. Change in magnetic properties of $\text{Fe}_{39}\text{Ni}_{39}\text{Si}_9\text{B}_{13}$ alloy after a plastic deformation at different temperatures: deformation 5%, $T = 240^\circ\text{C}$ (1), deformation 5%, $T = 260^\circ\text{C}$ (2), deformation 5%, $T = 275^\circ\text{C}$ (3)

sure of 125 kPa during the annealing in a relatively high temperature is shown in Fig. 5. It seems that the annealing after a plastic deformation significantly changes the nature of some magnetic parameters. These processes take place at the initial stage of annealing. The value of B_m remains constant, but the value of B_r decreases. A decrease in the values of H_c and the B_r/B_m ratio is noticeable. However, even if there is a decrease, these values are practically convenient. This suggests that the induced plastic deformation field, elastic stresses, and structural changes are conditioned by the atomic pair ordering and practically relaxed [14]. The development of structural relaxation processes in the selected temperature-time mode during the annealing does not depend on the previous processing of the material.

Figure 6 shows the temperature dependence of the operating magnetic parameters. As can be seen, there is no influence of the temperature on the operating magnetic parameters up to about 400°C . This effect starts after about 400°C . This fact determines that the maximum operating temperature inside

the devices made of the studied materials is about 400°C . This temperature is by 33% higher than the operating temperature range (up to 300°C) of 3% electric steel [21]. This fact also ensures that there will be no effect of the temperature on the application of amorphous materials in contactors with an operating temperature interval of $-5 + 70^\circ\text{C}$ [20]. The study of the processes that lead to the change of magnetic parameters during the annealing shows that defects caused by structural relaxation processes due to a deformation are completely annihilated at the beginning of the processing [15, 16]. This fact can be said on the basis of the coincidence of the results obtained after a plastic deformation with and without magnetic field (Fig. 6). However, structural changes as a result of the plastic deformation in the amorphous matrix, as well as the microcrystallization process, are weak. This affects a change of the magnetic properties.

It is known that the microcrystallization process takes place in an amorphous matrix during the annealing with and without magnetic field [15]. In this

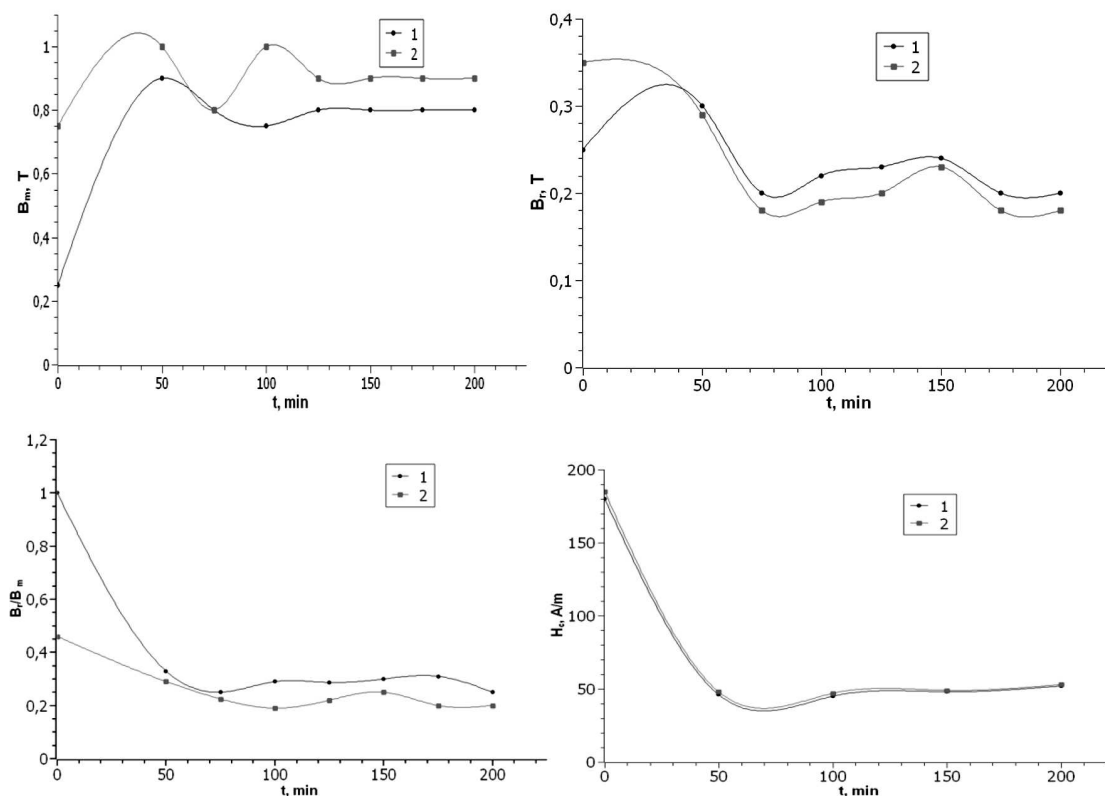


Fig. 6. Change of magnetic parameters in $Fe_{39}Ni_{39}Si_9B_{13}$ alloy during the annealing after a plastic deformation (75–125 kPa) at a high temperature (210 °C): ▲ – before the deformation, ● – after the deformation

case, the mechanism of the microcrystallisation process is the same. However, there is a dependence of the microcrystallisation degree on the annealing time. The growth rate of microcrystals formed during the annealing with and without magnetic field also decreases [17]. Based on the obtained results, we can define the experimental modes for a complex processing of materials as follows: keeping the amorphous specimen containing $Fe_{39}Ni_{39}Si_9B_{13}$ at 240 °C for 90 min in order to reduce stresses after a plastic deformation under the pressure of 75–125 kPa, then performing the thermal processing at a temperature of 360 °C, where the atomic pair ordering processes are activated due to the diffusion, below the Curie temperature, for 200 min in a magnetic field.

As a result of such processing, residual elastic stresses are released, and the amorphous-crystalline material with high magnetic properties is obtained. Therefore, the analysis of experimental processing modes of amorphous materials shows that the complex change of physical properties can be achieved not only

by the methods of induction of different types of magnetic anisotropy, but also by adjusting the formed amorphous crystal structure. In the table below, the specific properties of the amorphous $Fe_{39}Ni_{39}Si_9B_{13}$ specimen investigated in this study are compared with those of crystalline specimens of 3% electrical steel, which are now widely used in contactor cores.

As can be seen from Table 3, the studied materials differ from the currently used crystalline 3% electric steel in that the Curie temperature and saturation induction value are small, the density is low, the remagnetization losses are very small, and the specific electric resistance is very high. The crystalline electric steels which are widely used now have approached the limit of their application properties in terms of their magnetic properties.

Due to the great importance of electric machines and mechanisms in industry, it is necessary to apply new, for example, modern soft magnetic materials with amorphous and/or nanocrystalline structure. The advantages obtained as a result of replac-

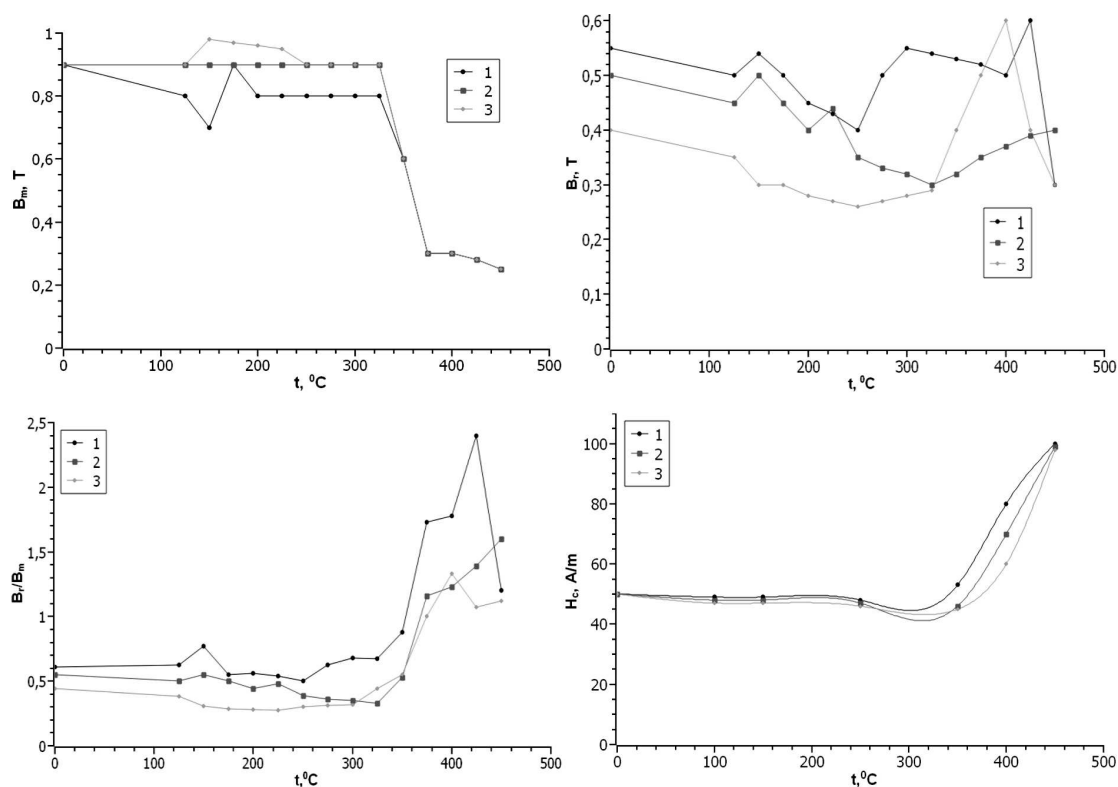


Fig. 7. Influence of processing mode and temperature on magnetic parameters of $\text{Fe}_{39}\text{Ni}_{39}\text{Si}_9\text{B}_{13}$ alloy: processing in magnetic field (1), processing without magnetic field (2), processing with cooling in magnetic field (3)

Table 3. Comparison of properties of the amorphous material and 3% electric steel

Materials	Properties						
	B_m , T	H_c , A/m	ρ , $10^{-8} \Omega\text{m}$	Thickness, mm	T_c , °C	P, W/kg	Density, g/cm^3
$\text{Fe}_{39}\text{Ni}_{39}\text{Si}_9\text{B}_{13}$ based amorphous layer	0.9	40–50	127	0.03	410	50 Hz 1.0 T $P = 0.8$	7.2
3% electrical steel	2.03	60–104	45	0.3	770	50 Hz $P = 1.2$ 1.0 T	7.68

ing the cores in contactors with amorphous materials are as follows.

1. Loss against eddy currents decreased by 1.5 times as a result of the 2.6-times-greater specific electric resistance.

2. The strength of the end parts increased by 3 times; as a result, the service life of the contactor increased by 10%.

3. As a result of the fact that amorphous materials are more resistant to the corrosion [18] compared to the electric steel, the use of contactors in humid environments has become more convenient.

4. The fact that the density of amorphous materials is less than 6% has led to the saving of these materials.

Based on the above, as well as on the results of different studies [19] carried out on different compounds,

we can say that this field has great prospects. However, one of the disadvantages of amorphous alloys is that they crystallize when heated to high temperatures. Therefore, for the stability of the products made of amorphous alloys, their temperature should not exceed the maximum operating temperature which is typical of each alloy.

The experiment was conducted on a Siemens 3Tf43-10 contactors of the currently widely used Reifenhäuser 801-1.90-33WT extrusion equipment. These contactors are rated for 5000 times connections by the manufacturer [20]. During the production verification, the 3% electric steel cores of these contactors were replaced with amorphous cores based on $\text{Fe}_{39}\text{Ni}_{39}\text{Si}_9\text{B}_{13}$ that we have studied. At this time, a 7% higher result than the factory resource (5350 times) was achieved. No signs of the corrosion or damage to the contact ends of the contactors were observed during the operation. This fact makes it possible to apply the studied material in the described field. High corrosion resistance and mechanical properties of amorphous cores ensure a reliable operation of these contactors in humid and aggressive environments, as well as in marine transport equipment and sensitive devices.

4. Conclusion

It is found that small changes in magnetic parameters during a deformation of the studied amorphous $\text{Fe}_{39}\text{Ni}_{39}\text{Si}_9\text{B}_{13}$ ribbons practically do not affect their operation mode. The change of magnetic parameters occurs at temperatures higher than 400 °C. This temperature is by 33% higher than the operating temperature range of 3% electric steel (up to 300 °C). From this, we can conclude that the operating temperature will not affect the operating magnetic parameters of the studied amorphous $\text{Fe}_{39}\text{Ni}_{39}\text{Si}_9\text{B}_{13}$ materials. Thus, it is more appropriate to replace the crystalline core of thermal control contactors with $\text{Fe}_{39}\text{Ni}_{39}\text{Si}_9\text{B}_{13}$ or other amorphous materials with similar properties.

1. H. Gavrilă, V. Ionita. Crystalline and amorphous soft magnetic materials and their applications – status of art and challenges. *J. Optoelectron. Adv. Mater.* **4** (2), 173 (2002).
2. C.T. Chang, B.L. Shen, A. Inoue. Co–Fe–B–Si–Nb bulk glassy alloys with superhigh strength and extremely low magnetostriction. *Appl. Phys. Lett.* **88** (1), 011901 (2003).
3. J.M. Dubois, P.H. Gaskell, G. Le Caer. Model for the structure of metallic glasses based on chemical twinning. *Proc.*

Royal Soc. of London A: Math., Phys. Engin. Sci. **402** (1823), 323 (1985).

4. V.E. Vavilov, O.A. Yushkova, Y.V. Rakhmanova *et al.* An ultra-high-speed starter-generator with a magnetic core of amorphous iron for unmanned aerial vehicles. *Russian Electrical Engineering* **89** (1), 13 (2018).
5. T.M. Panakhov, A.A. Isaeva, N.M. Rafiev, A.G. Guseinov. Magnetic thermocouples made of Co–Fe and Ni–Fe permalloys. *J. Tech. Phys.* **64** (7), 987 (2019).
6. A.A. Glaser, A.P. Potapov, E.V. Belozerov. Magnetic properties of amorphous alloys of the Co–Fe–Si–B systems with different contents of B. *Fiz. Met. Met.* **61** (5), 893 (1986).
7. T.K. Jeong, S.H. Hong, X. Bian, K.G. Prashanth. Effect of boron addition on thermal and mechanical properties of Co–Cr–Mo–C–(B) glass-forming alloys. *Intermetallics* **99**, 1 (2018).
8. S. Lesz, M. Nabiaek, R. Nowosielski. Structure and magnetic properties of $\text{Fe}_{56}\text{Co}_7\text{Ni}_7\text{B}_{20}\text{Nb}_{10}$ metallic glasses. *J. Achiev. Mater. Manufact. Engin.* **55** (2), (2012).
9. M. Akiba, B. Shen, A. Inoue. Bulk glassy Fe–Mo–Ga–P–C–B–Si alloys with high glass-forming ability and good soft magnetic properties. *Materials Transactions* **46** (12), 2773 (2005).
10. K. Gruszka, M. Nabialek, M. Szota *et al.* Analysis of the thermal and magnetic properties of amorphous $\text{Fe}_{61}\text{Co}_{10}\text{Zr}_{2.5}\text{Hf}_{2.5}\text{Me}_2\text{W}_2\text{B}_{20}$ (where Me = Mo, Nb, Ni OR Y) ribbons. *Arch. Metall. Mater.* **61** (2), 641 (2016).
11. Qianke Zhu, Shuling Zhang, Guihong Geng. Effects of annealing on the structure and magnetic properties of $\text{Fe}_{80}\text{B}_{20}$ magnetostrictive fibers. *J. Appl. Biomater. Funct. Mater.* **14** (Suppl 1), S56 (2016).
12. K. Suzuki, X. Fujimori, K. Hashimoto. *Amorphous Metals*. Edited by T. Masumoto (Metallurgy, 1987), pp. 150–156 (in Russian).
13. B.A. Kornienkov, M.A. Libman, B.V. Molotilov, D.I. Kadyshchev. Anomalous magnetic changes in amorphous Fe–Ni–Si–B alloy. *Allerton Press, Inc., Steel in Translation* **45** (3), 231 (2015).
14. Diao-Feng Li, Yong Shen, Jian Xu. Bending proof strength of $\text{Zr}_{61}\text{Ti}_2\text{Cu}_{25}\text{Al}_{12}$ bulk metallic glass and its correlation with shear banding initiation. *Intermetallics* **126**, 106915 (2020).
15. N.M. Rafiyev. Effects of heat treatment on some magnetic properties of amorphous alloys containing $(\text{Fe–Ni})_{1-x}\text{M}_x$ (M = Si, B). *J. Zeitschrift für Naturforschung A* **77**, 08 (2022).
16. H.B. Yu, X. Shen, Z. Wang *et al.* Tensile plasticity in metallic glasses with pronounced relaxations. *Phys. Rev. Lett.* **108**, 015504 (2012).
17. A.P. Abdullayev V.I. Ahmadov, A.A. Isayeva. Magnetic penetration investigation on the bands made of amorphous magnetically soft $(\text{CoFe})_{75}\text{Si}_{10}\text{B}_{15}$ alloys under the thermal processing. *Intern. J. Mod. Phys. B* **33** (3), (2020).
18. L. Velasco, J.J. Olaya1, S.E. Rodil. Effect of Si addition on the structure and corrosion behavior of NbN thin films de-

- posited by unbalanced magnetron sputtering. *Appl. Phys. A* **122**, 101 (2016).
19. N.I. Statsenko, K.A. Vasilchenko. The use of amorphous and nanocrystalline metal alloys in aircraft electrical machines. *Actual Problems of Aviation and Astronautics* **2** (2017).
 20. Low-voltage switchgear and controlgear. Standard number IEC 60947-4-1. Part 6.2. B.2.2. IEC-2018.
 21. Cheng-Ju Wu, Shih-Yu Lin, Shang-Chin Chou *et al.* Temperature effects on the magnetic properties of silicon-steel sheets using standardized toroidal frame. *Sci. World J.* Article ID 975051 (2014).
 22. ASTM A 927/A 927M-04, Standard Test Method for Alternating Current Magnetic Properties of Toroidal Core Specimens Using the Voltmeter-Ammeter-Wattmeter Method, American Society for Testing and Materials, West Conshohocken, Pa, USA, 2000.
 23. N.M. Rafiyev. Effects of heat treatment on some magnetic properties of amorphous alloys containing Fe₄₉Ni₂₉Si₉B₁₃ and Fe₅₉Ni₁₉Si₉B₁₃. *J. Phys. & Optics Sci.* **4** (3), 1 (2022).
 24. J.S. Langer. Shear-transformation-zone theory of deformation in metallic glasses. *Scripta Materialia* **54**, 375 (2006).

Received 30.12.22

Н.М. Рафієв, В.І. Ахмадов, А.А. Ісаєва

ПЕРСПЕКТИВИ ВИКОРИСТАННЯ
АМОРФНИХ Fe-Ni-Si-B СТРИЧОК
У ЯКОСТІ ОСЕРДЯ КОНТАКТОРІВ

Розглядається можливість використання аморфного матеріалу Fe-Ni-Si-B у якості осердя контакторів замість 3% електросталі з кристалічною структурою. Сплав Fe-Ni-Si-B перебував під дією механічного, термомеханічного та магнітного полів. Зразки було відпалено в олії при 360 °C в магнітному полі 200 А/м протягом 200 хв. Температурний режим вибирали таким чином, щоби під час відпалювання у матеріалі відбувалася релаксація напружень і спостерігалися контрольовані структурні зміни.

Ключові слова: аморфний магнітний сплав, обробка.